Fuel Processing Technology 230 (2022) 107217

Contents lists available at ScienceDirect

Fuel Processing Technology

journal homepage: www.elsevier.com/locate/fuproc

Low-rank coal pyrolysis polygeneration technology with semi-coke heat carrier based on the dual-fluidized bed to co-produce electricity, oil and chemical products: Process simulation and techno-economic evaluation

Yao Zhu, Kaikun Li, Qinhui Wang *, Jianmeng Cen, Mengxiang Fang, Zhongyang Luo

State Key Laboratory of Clean Energy Utilization, Zhejiang University, Hangzhou 310027, China

ARTICLE INFO

Keywords:
Low-rank coal
Dual-fluidized bed pyrolysis polygeneration
Semi-coke heat carrier
Techno-economic analysis
Environmental assessment

ABSTRACT

Pyrolysis polygeneration technology is a good way to realize clean and efficient utilization of low-rank coal and heat carrier is a key factor. Aspen Plus is used to establish low-rank coal pyrolysis staged conversion polygeneration technology with semi-coke heat carrier based on dual-fluidized bed (CPSCPC-DFB), which couples with ultra-supercritical semi-coke powder furnace for power generation. Three processes are simulated to co-produce methanol (CPSCPC-DFB-M), synthetic natural gas (CPSCPC-DFB-S) and hydrogen (CPSCPC-DFB-H). Mass and carbon balance are established, techno-economic, environmental and sensitivity analysis are carried out, and the comparison with ultra-supercritical coal-fired power plant (SCFP) is made. The results show that the comprehensive performances of CPSCPC-DFB-M, CPSCPC-DFB-S and CPSCPC-DFB-H are significantly better than those of SCFP in energy loss (49.37%, 47.33%, 45% and 55.6%), CO_2 emissions (2.07, 2.12, 2.22 and 2.52 kg/kg_{coal}), internal rate of return (23.24%, 21.83%, 29.52% and 17.56%). Although the total investment of CPSCPC-DFB is much higher than SCFP, the net present value is better than SCFP. Comparing the three polygeneration systems, the total investment and CO_2 emissions of CPSCPC-DFB-H are slightly higher than those of other two systems, but CPSCPC-DFB-H has absolute advantages in economy. Sensitivity analysis shows that the anti-risk ability of the polygeneration systems are significantly improved.

1. Introduction

In 2019, foreign dependence ratio of oil and natural gas in China are 70.8% and 43% respectively, posing a major challenge to China's energy security [1]. In the future, fossils fuel still accounts for a very high proportion of 79.5% [2], and coal will still play an important role in China for a long time and occupy a considerable share in electricity and heat production [3], which makes the CO_2 emission the largest in the world [4,5]. China strives to get carbon neutral by 2060 [6]. In this context, the obsolescence or transformation of coal-fired power plants is a worldwide problem. Direct obsolescence will cause waste, so it is better to transform the existing power units and realize clean power generation. Coal staged conversion polygeneration technology (CSCP) has attracted much attention because it can co-produce power and chemical products with significant benefits of energy saving and emission reduction [7,8].

Nomenclature

CP	price of coal
MP	methanol prices
CPP	price of crude phenol
NP	naphtha prices
DP	diesel prices
EP	electricity prices
ART	annual operating hours
SNGP	price of SNG
H_2P	price of H_2
SNG	synthetic natural gas
C_{RM}	raw material costs
C_{DW}	direct wages
CO_{DE}	other direct expenses
C_{MC}	manufacturing costs
C_{ME}	management expenses
C_{SE}	sales expenses

* Corresponding author.
E-mail address: qhwang@zju.edu.cn (Q. Wang).

https://doi.org/10.1016/j.fuproc.2022.107217
Received 31 December 2021; Received in revised form 17 February 2022; Accepted 18 February 2022
Available online 2 March 2022

C_{FE} financial expenses

Abbreviations

TPC total production costs
TCI total capital investment
FCI fixed capital investment
LII loan interest invested
SMR methane steam reforming
PSA pressure swing adsorption
WGS water gas shift
WCI working capital
IRR internal rate of return
PP payback period
SPP static payback period
DPP dynamic payback period
NPV net present value
DFBP dual-fluidized bed pyrolysis unit
SSPP 660 MW ultra-supercritical semi-coke powder furnace for power generation unit
SEDE selexol unit
MESP methanol synthesis purification unit
PSA-H_2 hydrogen extraction by pressure swing adsorption
PSA-CO_2 pressure swing adsorption carbon dioxide extraction
PSA-CH_4 methane extraction by pressure swing adsorption
TAHY tar hydrogenation unit
PAR phenol ammonia recovery unit
CSCP coal staged conversion polygeneration technology
SCFP the ultra-supercritical coal-fired power plant of the same power generation scale
CPSCPC-DFB the low-rank coal pyrolysis staged conversion polygeneration technology with semi-coke heat carrier based on dual-fluidized bed

At present, CSCP is mainly divided into two categories based on pyrolysis and gasification [9]. Table 1 summarizes the researches on polygeneration in recent years. It is found that there are more researches on coal gasification polygeneration technology, which is attributed to the development of integrated gasification combined cycle and the demand for chemical products. Coal can be converted into high-quality syngas through gasification [10]. Syngas can be used not only for power generation, but also as an intermediate product of synthetic chemical products [11,12]. However, oil and gas products cannot be obtained at the same time in gasification process, and for low-rank coal with high volatile, gasification will make volatile content cannot be effectively utilized [13]. Pyrolysis can extract valuable volatiles from coal to co-produce oil and chemicals before gasification or combustion. Therefore, coal pyrolysis polygeneration technology is a better way to realize clean and efficient utilization of low-rank coal at present [9,14]. The storage proportion of low-rank coal in China exceeds 55% [5], which is the most suitable coal for pyrolysis according to its physical and chemical characteristics [6]. Hence, the pyrolysis of low-rank coal will attract more and more attention [15,16].

Table 1
The researches on polygeneration system.

Basis of polygeneration systems	Co-produced products	Ref.
Biomass gasification	Dimethyl ether	[17]
Coal gasification	H_2 and electricity	[18]
Refuse derived fuel gasification	Dimethyl ether and electricity	[19]
Coal gasification	Syngas and electricity	[20]
Coal gasification	Methanol and electricity	[8]
Coal gasification	Ethylene glycol and dimethyl ethers	[21]
Coal gasification	Methanol and electricity	[22]
Coal gasification	Synthetic natural gas and electricity	[23]
Coal gasification	Synthetic natural gas and methanol	[24]
Coal gasification	Methanol and ethylene glycol	[25]
Biomass gasification	Ethylene glycol	[26]
Coal pyrolysis coupled with combustion	Liquid fuel, synthetic natural gas and electricity	[9]
Coal pyrolysis coupled with gasification	Tar, gasified gas and electricity	[13]
Coal pyrolysis–gasification–combustion	Methanol, oil and electricity	[14]

The heat source for coal pyrolysis is the core issue that affects the composition and distribution of products [27]. The existing heat sources include gas and solid heat carrier [28]. The gas heat carrier is usually high temperature flue gas containing a lot of O_2 and N_2 so that the gas quality is poor. The solid heat carriers include semi-coke, ash and quartz sand, which can avoid the pollution of pyrolysis gas and have obvious advantages [29,30]. As one of the pyrolysis products, semi-coke has been widely concerned for its advantages of no regeneration and improving the quality of light tar [31–33]. However, most of the existing researches are based on two-stage or multi-stage reactors, focusing on the catalytic cracking of semi-coke on volatile matter [28,29,31]. The research on dual-fluidized bed pyrolysis with semi-coke heat carrier is not sufficient, and the whole process analysis and feasibility analysis of system and the subsequent deep processing of products are lacking. Secondly, it can be seen from Table 1 that the analysis of pyrolysis polygeneration system with semi-coke heat carrier has not been reported in literatures. It is necessary to carry out the simulation of this part to provide reference for the large-scale industrial promotion and application of the CPSCPC-DFB.

To solve the above problems, based on the basis of 1MWt experiment, Aspen Plus is used to establish the whole process simulation and global technical and economic analysis of CPSCPC-DFB, which couples with 2 × 660 MW ultra-supercritical semi-coke powder furnace for power generation. According to market demand and gas deep processing route, three polygeneration processes are simulated to co-produce crude phenol, naphtha, diesel, electricity and methanol (CPSCPC-DFB-M)/ SNG (CPSCPC-DFB-S)/ H_2 (CPSCPC-DFB-H) respectively. The mass and carbon balance of the system is established to discuss the feasibility of the system. The technical, economic and environmental performance of different systems are compared. Through sensitivity analysis, the influence of different parameters on internal rate of return (IRR) of the system is obtained. The polygeneration systems are compared with the SCFP to provide technical support and comprehensive feasibility evaluation for the application and promotion of the CPSCPC-DFB in the next step. The specific content is shown in Fig. 1.

Whether it is reformed or newly built, the polygeneration technologies of pyrolysis coupled combustion or gasification coupled combustion must be combined with a circulating fluidized bed boiler to operate. With high-temperature ash as the heat carrier, the dedusting load of pyrolysis gas is large and the ash content of tar is relatively high. The dual-fluidized bed pyrolysis polygeneration technology proposed in this work does not require a coupled power boiler and can be arranged in any position in principle. Semi-coke can be used for power generation and also other purposes. This work has the following three innovations. First, a dual-fluidized bed pyrolysis simulation system for low-rank coal with semi-coke heat carrier is established. Second, semi-coke is used for power generation. The system co-produces electricity, oil and chemical products, realizes clean and efficient utilization of low-rank coal, and solves the problem of energy imbalance in our country. Third, this work proposes and simulates three systems, and compares them with direct power generation technology to choose the best system under different conditions and achieve economic optimization.

2. Processes and model methods

2.1. Processes introduction

The three processes are shown in Fig. 2. The whole system includes

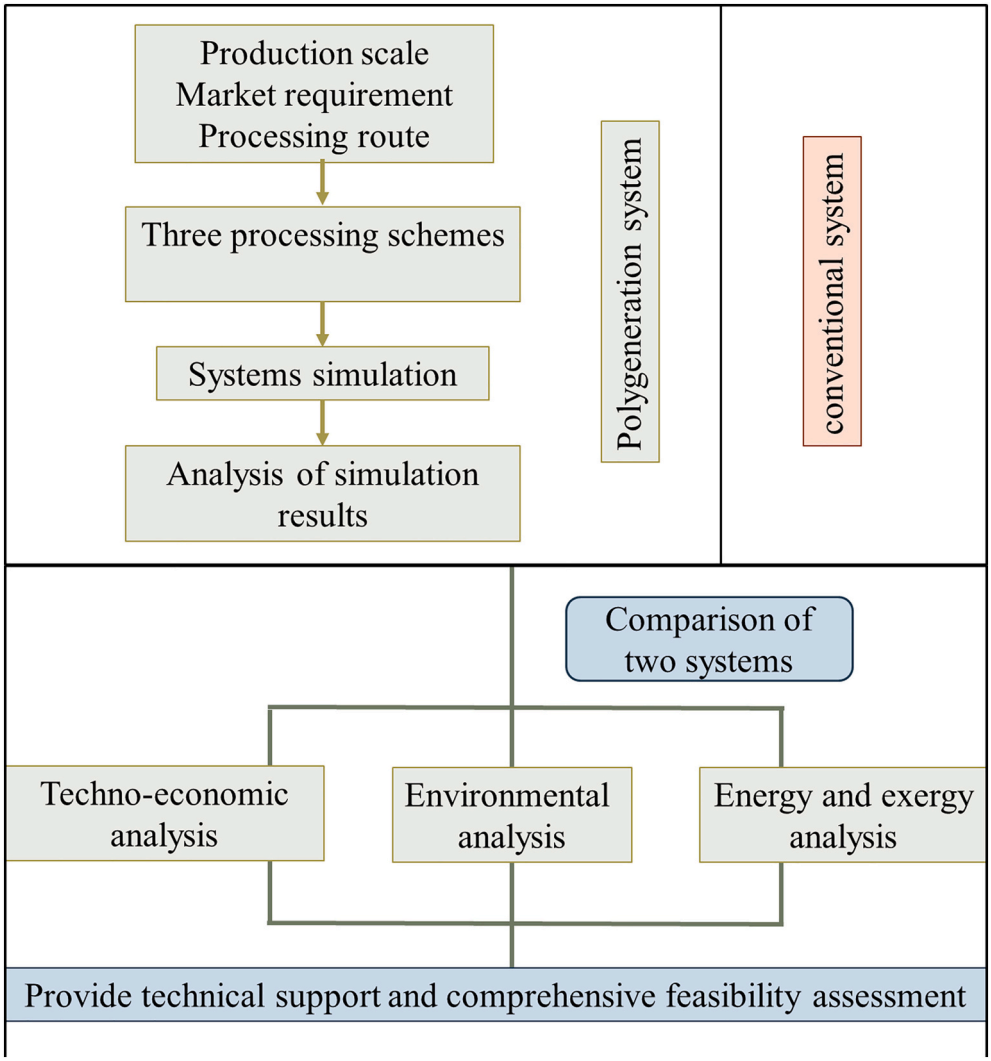

Fig. 1. Systematic analysis process.

pyrolysis part, power generation part, liquid production part, and gas processing part. In the above three processes, except for the difference in the gas processing part, the other parts are kept consistent for comparison. The pyrolysis part includes mainly DFBP unit, the most important in which is the circulation path of the semi-coke heat carrier. The power generation part consists of SSPP and corresponding steam-water unit. The gas processing part of CPSCPC-DFB-M consists of SEDE, SMR, MESP and PSA-H_2 unit. The gas processing part of CPSCPC-DFB-S is mainly composed of SEDE, SMR, WGS, PSA-CO_2, PSA-CH_4 and PSA-H_2 unit. In process of CPSCPC-DFB-H, the coal gas purified passes through the SMR, WGS, and PSA-CO_2 unit. Finally, H_2 is separated through the PSA unit, part of which is input to the TAHY unit, and the rest is output as the product.

In this work, Aspen Plus is used to carry out the whole process simulation for the above three processes and compares from different aspects to select the better process. Because the pyrolysis process is very complicated, some assumptions are proposed to simplify the simulation reasonably, as shown in Table A1 [14,34].

2.2. Experiment

The proximate and element analyses of Runbei coal and char are shown in Table 2. In order to obtain the data required for the simulation process, relevant experiments and analyses are carried out on a 1MWt dual-fluidized bed. The 1MWt dual-fluidized bed coal staged conversion pilot plant mainly consists of semi-coke combustion heating furnace, fluidized bed pyrolysis furnace, steam-water system, coal gas crude purification system, fuel feed system, and control system. The total height of pyrolysis furnace and heating furnace is 7.2 m and 11.2 m respectively, and the feeding mass of coal is 138 kg/h. The specific operation steps and working condition are given in Supplementary material. The data in Tables 2–4 were obtained from 1MWt pilot test data at pyrolysis temperature of 630 °C. The results of products and components are shown in Table 3. The composition of coal tar pitch elements and hydrogenation products are shown in Table 4.

2.3. Unit description

2.3.1. Pyrolysis part

The DFBP unit mainly includes a fluidized bed pyrolysis furnace and a circulating fluidized bed semi-coke heating furnace, as shown in Fig. 3. In actual process, there is a stable material circulation between the pyrolysis furnace and the semi-coke heating furnace, and it is impossible to distinguish semi-coke product and semi-coke heat carrier. Therefore, a new solution is proposed in this work, that is to define a new NC component named Charshc, whose element composition is consistent with that of semi-coke, which is connected to the heating furnace through heat flow and transfers the heat between the two beds. The semi-coke is separated into semi-coke product and semi-coke heat carrier by Charshc-sep. The semi-coke product is separated by Char-sep,

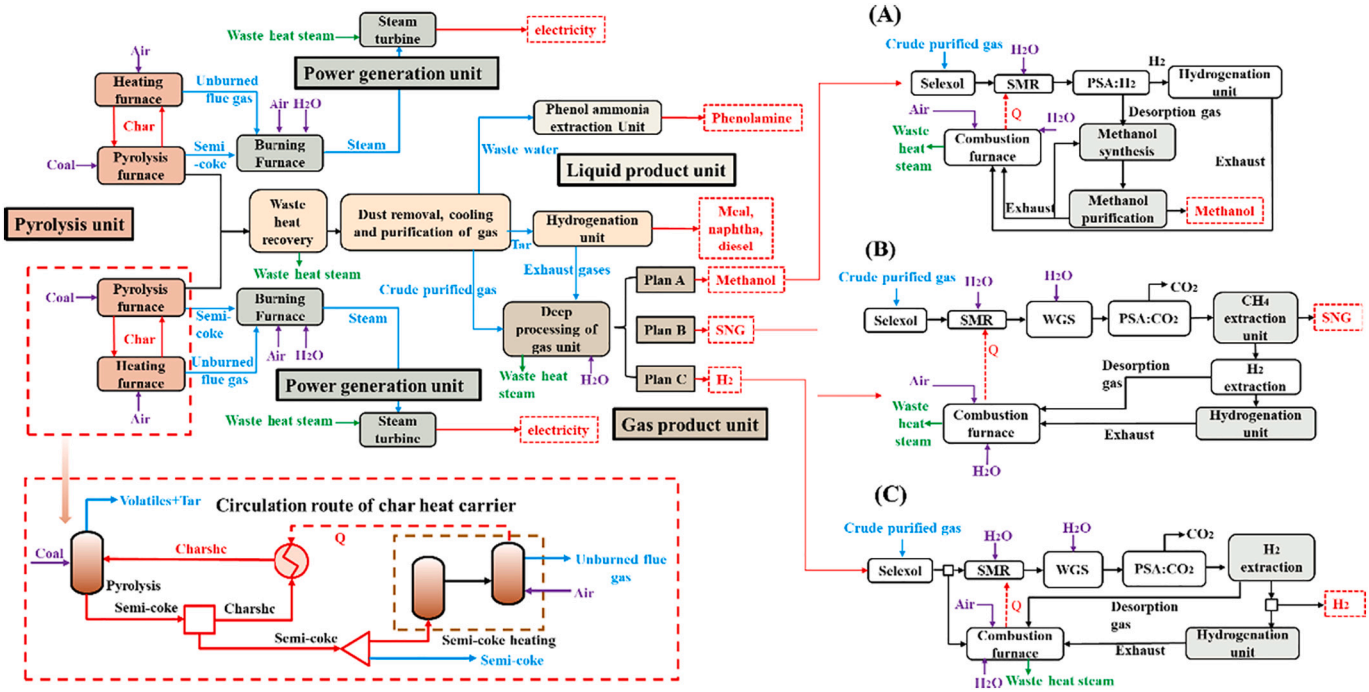

Fig. 2. Schematic flow diagram of the polygeneration system.

Table 2
Proximate analysis and elemental analysis of coal and char.

Sample	Proximate analysis, ad%				Element analysis, ad%					Heat
	M	A	V	FC	C	H	N	S	O	Qnet(MJ/kg)
Coal	5.61	6.64	36.98	50.77	70.3	4.43	1.08	0.81	11.13	27.733
Char	0	10.63	11.67	77.7	83.45	1.61	0.68	0.22	3.41	29.736

Table 3
Product and component distribution.

	Component	Mass fraction/%		Component	Mass fraction/%
Char	/	63.74		CO_2	3.3
	C_6H_6O	1.61		C_2H_4	0.81
	$C_{16}H_{34}$	2.16		C_2H_6	1.35
Tar	C_9H_7N	1.6		C_3H_6	0.7
	$C_{10}H_8$	4.46		C_3H_8	0.3
	$C_{12}H_8S$	1.61	Gas	NH_3	0.09
	H_2O	10.4		H_2S	0.12
Gas	H_2	0.3		N_2	0.57
	CH_4	4.29		O_2	0.07
	CO	2.52		/	/

Table 4
Element composition of tar pitch and component distribution of hydrogenation products.

Asphalt	Element/wt %	Component distribution of hydrogenation products	Mass fraction /%
C	92	Diesel	42.53
H	5.5	Naphtha	28.36
N	1	Crude phenol	15.26
S	0.8	Asphalt	3.54
O	0.7	C1-C4	7.89
–	–	H_2O	0.71
–	–	H_2S	1.01
–	–	NH_3	0.7

and part of that enters the semi-coke heating furnace for combustion to provide the heat required by the semi-coke heat carrier. In the pyrolysis furnace, it is defined as an inert component and only provides heat as a heat carrier. The circulation path of the semi-coke heat carrier shown by the red line in Fig. 3 is a key.

2.3.2. Power generation part

The semi-coke produced by pyrolysis in this work is used for combustion and power generation, so DFBP unit couples with SSPP and corresponding steam-water unit. The flue gas produced after the combustion of the pyrolysis semi-coke exchanges heat through the tail flue and the economizer to produce 600 °C/28 MPa ultra-supercritical steam for power generation. The simulation process is shown in Fig. A1. Heater and Compr is used to simulate heat exchange equipment and pneumatic cylinders, respectively. The simulation results of the power generation part are shown in Table A2.

2.3.3. Liquid product part

Tar hydrogenation is one of the important processes of clean and efficient utilization of coal. This work adopts tar hydrogenation technology with heterogeneous suspended bed [35]. First, the tar is distilled to extract phenol to obtain the phenol with a boiling point less than 230 °C and a de-phenolic oil with a boiling point of 230–350 °C. Then, hydrocatalytic cracking of heavy oil with boiling point over 350 °C is carried out in heterogeneous suspended bed. The simulation process of tar hydrogenation is shown in Fig. A2 after appropriate simplification.

2.3.4. Gas product part

The H_2S in the crude purified gas is removed by SEDE unit, and the

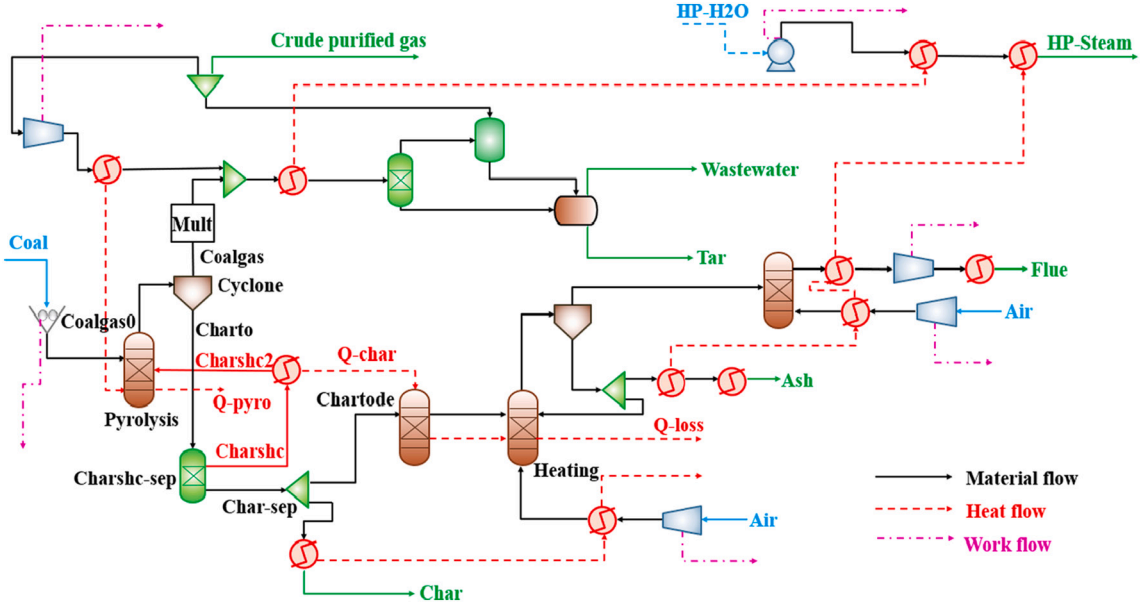

Fig. 3. The DFBP unit.

H_2S-rich acid gas is used to produce sulfur. The hydrogen-carbon ratio required for methanol synthesis is 2.0–2.2, and the tar hydrogenation also consumes a large amount of H_2. In order to meet the demand of H_2, CH_4 in the coal gas is converted by methane steam reforming. The desulfurized coal gas enters the SMR unit to adjust the hydrogen-carbon ratio. The heat required for reforming comes from the combustion of exhaust gas of each unit. The WGS unit is used to adjust the ratio of CO and H_2 in the coal gas after steam methane reforming. According to different processes, PSA unit such as CO_2 removal, CH_4 or H_2 extraction are established. The gas with a hydrogen-carbon ratio of 2 from the SMR unit is mixed with the circulating tail gas and enters the synthesis tower for reaction. The obtained crude methanol is cooled by multiple stages and separated into gas components. Part of the gas enters the PSA unit, and the remaining part is recycled back to the synthesis tower. The liquid component of the flash column is purified in the distillation column, and the distillate at the bottom of the column is the high concentration methanol product.

The above simulation process is shown in Figs. A3–5 respectively. Table 5 summarizes reactions involved in the gas product part. The expression of reaction rates and the values of kinetic are referred to [11,36] and shown in Table A3.

Tables 6–7 and Table A4 respectively give the main process parameters of each model, physical property methods and related design specifications, respectively.

Table 5
Reactions involved in the gas product part.

Reactions	Number	Ref.
SEDE		
$H_2S + \frac{3}{2}O_2 \rightarrow SO_2 + H_2O$	(1)	
$2H_2S + SO_2 \rightarrow 2H_2O + 3S(s)$	(2)	[24]
$SO_2 + 3H_2 \rightarrow H_2S + 2H_2O$	(3)	
$2H_2S + O_2 \rightarrow 2H_2O + 2S(s)$	(4)	
SMR		
$CH_4 + H_2O = CO + 3H_2$ $\Delta H = 206.12$ MJ/kmol	(5)	[37]
WGS		
$CO + H_2O = CO_2 + H_2$ $\Delta H = -41$ MJ/kmol	(6)	[36]
MESP		
$CO_2 + 3H_2 \leftrightarrow CH_3OH + H_2O$ $\Delta H = -49.43$ MJ/kmol	(7)	[36]
$CO_2 + H_2 \leftrightarrow CO + H_2O$ $\Delta H = 41.12$ MJ/kmol	(8)	

2.4. Calculation method

2.4.1. Energy and exergy efficiency evaluation

The calculation method of exergy is shown in the Supplementary material [38,39]. Energy and exergy efficiency are adopted to measure the utilization rate of input energy and exergy by the system, and the calculation formulas are as follows [24,40]:

$$\eta_{Energy} = \frac{\sum_i^n F_i En_i + W_{Electricity-out}}{F_{Coal} En_{coal} + W_{Electricity-in}} \times 100\% \quad (9)$$

$$\varepsilon_{Exergy} = \frac{\sum_i^n F_i Ex_i + W_{Electricity-out}}{F_{Coal} Ex_{coal} + W_{Electricity-in} + Ex_{Air}} \times 100\% \quad (10)$$

where, η_{Energy} and ε_{Exergy} represent the energy and exergy efficiency of the system respectively, %; F_i represents the molar flow of product i; F_{Coal} represents the coal feed mass, t/h; En_i and En_{coal} represent the energy carried by product i and coal respectively, which are low calorific values; $W_{Electricity-in/out}$ is the power consumption or power generation of the system. Ex_i and Ex_{Coal} represent the exergy carried by product i and coal respectively.

2.4.2. Technical and economic evaluation

2.4.2.1. Total capital investment (TCI). TCI is the sum of fixed capital investment (FCI), loan interest invested (LII) and working capital (WCI) during project construction. TCI can be calculated by the following formulas [21,41]. The equipment investment benchmark table of this project is shown in Tables A5–7.

$$FCI = \sum_{j=0}^{m} EI = \sum_{j=0}^{m} \left[EI_{r,j} \times \left(\frac{S_j}{S_{r,j}} \right)^{b_j} \right] \quad (11)$$

$$TCI = FCI + LII + WCI \quad (12)$$

where, EI, S_j and b_j represent the capital investment, equipment scale and scale factor of equipment j under the current scale; $EI_{r,j}$ and $S_{r,j}$ represent the purchase price and equipment scale of equipment j under the reference scale, respectively. Working capital take 20% of the FCI.

2.4.2.2. Total production costs (TPC). TPC includes production costs and general expenses. General expenses include management expenses,

Table 6
Design parameters of blocks used in Aspen plus flowsheet.

Unit	Model	Parameter setting of the key unit
DFBP	1. Pyrolysis: Ryield	1. The pyrolysis condition is 630 °C at 0.1 MPa. The pyrolysis products are derived from pyrolysis experiments.
	2. Heating: Ryield and RGibbs	2. Ryield to decompose the char into its constituent elements through calculator block. The RGibbs temperature is 900 °C and the heat loss is set at 1% controlled by the design specification.
	3. Cyclone	3. The separation efficiency is 99%.
	4. Heater	4. The air is heated to 350 °C and the flow rate is regulated using design specifications.
	5. Semi-coke separator: Char-sep	5. Semi-coke heat carrier proportion is adjusted by design specification.
SSPP	1. Burner: RGibbs	1. The combust condition is 1150 °C and 0.1 MPa.
	2. Air Heater: Heater	2. Heating of air required for combustor to 255 °C, the oxygen concentration of flue gas at the outlet controlled by the design specification.
	3. Steam Turbine	3. The HP-steam inlet temperature and pressure are 600 °C and 28 MPa respectively. The HP-steam flow is 1840 t/h and the rated power generation is 660 MW.
	4. Compr	4. Isentropic efficiency and mechanical efficiency are set to 0.92 and 0.98 respectively.
TAHY	1. Dephenol of tar and distillation of: RadFrac	1. Distillation flow rate and reflux ratio are 131.7kmol/h and 5.
	2. Hydrogenation reaction: Ryield	2. The temperature and the pressure are 440 °C and 19 MPa. The product distribution is obtained from experiment. The mass ratio of H_2 to tar at the entrance of hydrogenation reactor is set at 5:100.
	3. Tar and hydrogen compression: Pump and Compr	3. Isentropic efficiency is set to 0.8 and mechanical efficiency is set to 0.9.
SMR	1. Reforming tower: REquil	1. The pressure is 0.1 MPa and the temperature is 900 °C
	2. Tail gas combustion: RGibbs	2. The temperature is 950 °C and the air volume is regulated according to the design specification.
WGS	Two-stage transformation reaction: REquil	The equilibrium temperature difference is set to 25 °C and 10 °C respectively, and the molar ratio of H_2O/CO is 2:1.
MESP	1. Methanol synthesis tower: Rplug	1. The reaction process is controlled by LHHW kinetics equation. The reaction pressure is 6.97 MPa, and the temperature is 200-300 °C. The synthetic tower is a multi-tubular reactor with 3240 main pipes, 8 m pipe length and 0.04 m inner diameter.
	2. Methanol distillation column: RadFrac	2. The number of trays is set to 20, the reflux ratio is set to 5, and the flow rate at the bottom of the tower is determined according to the optimization of methanol concentration.
	3. Flash tower: Flash	

Table 7
Physical property methods.

Unit	Physical property methods
DFBP	PR-BM
SSPP	PR-BM and STEAM-TA
SEDE	PR-BM
TAHY	BK10 and SRK
SMR	NRTL
WGS	PR-BM
PSA	PR-BM
MESP	SRK and STEAM-TA

sales expenses and financial expenses. The calculation formula is as follows [25]:

$$TPC = C_{PC} + C_{ME} + C_{SE} + C_{FE} \tag{13}$$

$$C_{PC} = C_{RM} + C_{DW} + CO_{DE} + C_{MC} - C_{byproduct} \tag{14}$$

$$TPC = C_{RM} + C_{DW} + CO_{DE} + C_{MC} + C_{ME} + C_{SE} + C_{FE} - C_{byproduct} \tag{15}$$

where, C_{PC}, C_{RM}, C_{DW}, CO_{DE}, C_{MC}, C_{ME}, C_{SE}, C_{FE} *and* $C_{byproduct}$ represents production costs, raw material costs, direct wages, other direct expenses, manufacturing costs, management expenses, sales expenses, financial expenses and additional products. Table A8 shows the relevant assumptions and product tax-included prices used in the technical and economic analysis of this work [42]. C_{RM} includes raw materials and fuel power costs. C_{DW} and CO_{DE} include wages, bonuses and other subsidies and benefits, and benefits are calculated at 14% of C_{DW}. C_{MC} includes depreciation of fixed assets, equipment maintenance costs and workshop management costs. Workshop management and maintenance fees are 0.50% and 3.50% of the FCI respectively [9,14].

2.4.2.3. Net present value (NPV). NPV refers to the difference between the value of cash inflow and the value of cash outflow over the life of the plant, reflecting the profitability of the project during the life cycle. NPV greater than zero indicates that the project is economically feasible. The calculation formula is as follows [43]:

$$\sum_{t=0}^{n} CF_t(1 + IRR)^t = 0 \tag{16}$$

$$NPV = \sum_{t=0}^{n} CF_t(1 + i)^{-t} \tag{17}$$

where, IRR is the internal rate of return. When IRR $\geq$ i, it indicates that the project has reached the lowest level, and i is the discount rate which is taken as 8% [34]. CF_t represents the net cash flow of the t year and n is the life of the plant.

2.4.2.4. Payback period (PP). The static payback period (SPP) and dynamic payback period (DPP) are used to estimate the time required for total investment return, with DPP taking into account the time value of money [9]. The calculation formula is as follows:

$$SPP = A_1 + \frac{\sum_{t=0}^{A_1} B_t}{C_1} \tag{18}$$

$$DPP = A + \frac{\sum_{t=0}^{A} B_t(1 + i)^{-t}}{C} \tag{19}$$

where, A_1 and A respectively represent the last year in which the net cash flow and net present value are negative. Bt is the net cash flow in year t. C_1 and C respectively represent the annual net cash flow of the next year after A_1 and the net present value of the next year after A.

2.5. Environmental assessment

The impact and damage of various pollutants on the environment are different. Five impact categories are considered in this work, which are global warming, acidification, photochemical ozone formation, wastewater, and solid waste. In order to assess the comprehensive economic and environmental performance of the system, the environmental assessment of pollutant emissions is calculated by monetary environmental value, and the environmental cost of the system is calculated as follows [44]:

$$PE = \frac{\sum_{r=1}^{R}\sum_{n=1}^{N}\sum_{m=1}^{M} W(n,m)\bullet PWR(m,r)}{W_{coal}} \quad (20)$$

where *PE* is the environmental cost per ton of coal consumed, RMB/t_{coal}; *W(n,m)* is the amount of the *m* pollutant emissions in the *n* process, $t_{pollutant}$/h; *PWR(m,r)* is the monetary value of the *r* impact category of the *m* pollutant, RMB/$t_{pollutant}$; W_{coal} is the amount of coal input in the process, t_{coal}/h.

And this work compares the CO_2 emissions of the polygeneration systems and SCFP. Since the amount of coal input and product in the process is inconsistent, this work analyzes the CO_2 generated per kg of coal as the unit.

3. Results and discussion

3.1. The influence of key operating parameters of the system

3.1.1. Calculation of the semi-coke heat carrier circulation

The calculation of semi-coke heat carrier circulation is one of the key points in this work. There are two determinants of semi-coke heat carrier circulation: (1) The semi-coke heat carrier entering the heating furnace burns to 900 °C under anoxic conditions; (2) The heat carried by the semi-coke heat carrier must meet the heat demand of the pyrolysis furnace. Therefore, the flow rate of Charshc is adjusted by design specifications to make the pyrolysis furnace adiabatic, that is, all the heat required for pyrolysis comes from the high-temperature semi-coke heat carrier. The simulation results are shown in Table A9, which demonstrate that the separation rate of semi-coke is 0.16, the heat transferred from the heating furnace to the pyrolysis furnace through Charshc is 169.29 MW, and the total energy input from coal is 2418.93 MW. The heat required for pyrolysis accounts for 7.00% of the total heat input of coal, which is basically consistent with the literature [13], indicating that the established model meets the energy requirements of pyrolysis process in terms of thermodynamics.

3.1.2. Effects of different distillate rates and reflux ratios on tar yield in tar hydrogenation

Optimize the distillate rate and reflux ratio of the distillation column by using the design function of software, so as to obtain as much high purity naphtha and diesel oil as possible. The setting parameter and final simulation results are shown in Tables A10–11.

3.1.3. Temperature optimization of methanol synthesis tower

Fig. A6 shows the changes in methanol yield, net power generation and energy efficiency of the system within the temperature of the methanol synthesis tower at 180-280 °C. It can be found that the methanol yield has a great influence on the overall performance of the system. As the temperature of the synthesis tower increases, the methanol yield first increases and then decreases, which is attributed to the fact that high temperature is not conducive to the forward exothermic reaction. The reaction rate is slower at lower temperatures, indicating that the RPlug model can simultaneously simulate the effects of kinetics and thermodynamics on the reaction process. The variation trend of system energy efficiency and net power generation was positively correlated with methanol yield, and both reached the peak value at 230 °C. This is because when the methanol yield is high, the proportion of circulating exhaust gas and the power consumption of pressurization reduces, the net power generation of the system increases, and the overall energy efficiency improves.

3.2. The analysis of technical properties

3.2.1. Analysis of simulation results

The streams input and output of the four processes are shown in Table 8. It can be found that due to the co-production of methanol/SNG/H_2 and crude phenol, naphtha, diesel and other chemicals at the same time of power generation, the annual coal consumption of polygeneration systems is 1.31 million tons more than that of the ultra-supercritical power plant, but it brings more products and energy output.

Table 8
The results of system simulation.

	CPSCPC-DFB-M	CPSCPC-DFB-S	CPSCPC-DFB-H	2 × 660 MW ultra-supercritical power plant
		Fuel consumption		
Coal (million tons/year)	3.14	3.14	3.14	1.83
		Product yield		
Methanol (10^4 tons/year)	32.68	/	/	/
SNG (10^4 bids per/year)	/	17,849.56	/	/
H_2 (10^4 tons/year)	/	/	8.81	/
Crude phenol (10^4 tons/year)	5.17	5.17	5.17	/
Naphtha (10^4 tons/year)	12.40	12.40	12.40	/
Diesel (10^4 tons/year)	15.73	15.73	15.73	/
Electricity (KW/year)	6.57×10^9	7.23×10^9	6.46×10^9	6.26×10^9
CO_2 emissions (kg/kg_{coal})	2.07	2.12	2.22	2.52

3.2.2. Mass balance and carbon balance

Before calculating the energy efficiency, the mass flow and carbon flow of three processes are constructed. As shown in Fig. 4. Take CPSCPC-DFB-M as an example. The input coal of 628 t/h is converted into 336 t/h char, 93.8 t/h crude purification gas and 71.7 t/h tar. The 71.7 t/h of tar and 3.1 t/h of H_2 output from the PSA-H_2 unit enter the TAHY unit, resulting in 69 t/h of oil products. The tail gas of 5.5 t/h produced in the TAHY unit enters the MESP unit and burns to provide the required heat for reforming. The 93.8 t/h of crude purification gas enters the SEDE unit, and the obtained 69 t/h deacidification gas, 222.4 t/h of water vapor and 501.4 t/h of air enter the SMR unit to adjust the hydrogen-carbon ratio, and 148 t/h of effective syngas is obtained. The syngas enters the PSA-H_2 unit to generate 3.1 t/h H_2 into the TAHY unit and 144.7 t/h gas into the MESP unit to synthesize methanol. Finally, 79.9 t/h methanol product is obtained, and 59.7 t/h tail gas is burned into the reforming unit to provide heat.

The carbon balance analysis is shown in Fig. 4(a). The total amount of carbon input is 467.7 t/h from coal, which is effectively distributed in char, gas and tar, with the content of 280.4 t/h, 57.1 t/h and 62.8 t/h, respectively. Finally, 26.5 t/h of carbon in gas is stored in methanol, and 58.3 t/h of carbon in tar is stored in oil. Most of the carbon exists in the tail gas, mainly because the char yield from pyrolysis is the largest. The char is burned to generate electricity, and carbon is emitted with the exhaust gas in the form of CO_2. In summary, the mass and carbon are basically balanced during the simulation process, and the simulation results are credible.

3.2.3. Energy and exergy efficiency analysis

The exergy distribution and exergy efficiency of the system are shown in the Fig. 5. The results show that the difference in the consumption of the three polygeneration processes is attributed to the power consumption of the auxiliary machines, and the total power consumption of CPSCPC-DFB-M, CPSCPC-DFB-S and CPSCPC-DFB-H is 244.72, 150.69 and 200.10 MW respectively. The power consumption of each auxiliary machine is shown in the pie chart and that of CPSCPC-DFB-M is the largest, mainly due to the high-power consumption of

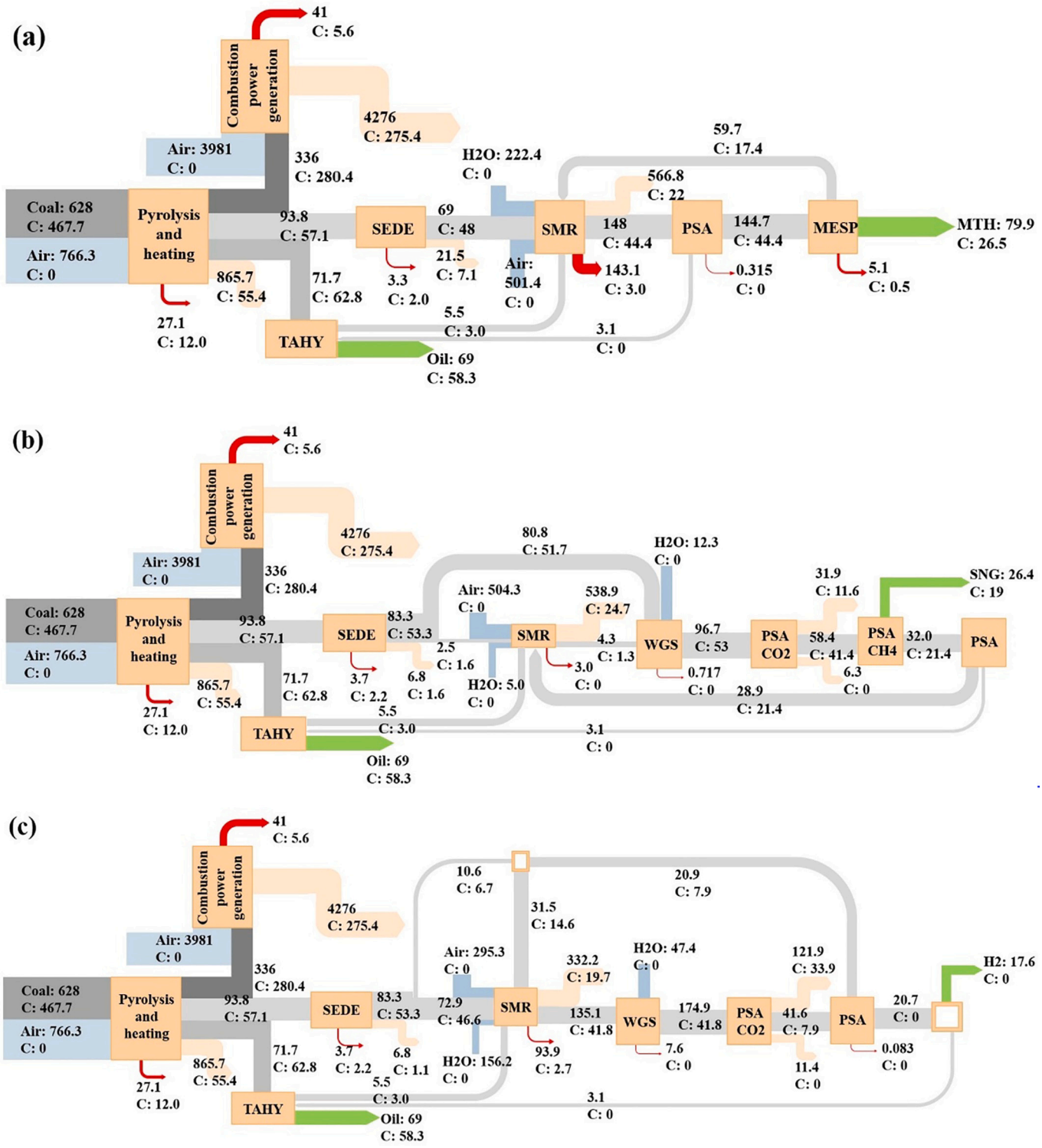

Fig. 4. Mass balance and carbon balance diagram (unit: t/h) (a) CPSCPC-DFB-M, (b) CPSCPC-DFB-S, (c) CPSCPC-DFB-H.

the MESP unit. The power consumption of CPSCPC-DFB-H is mainly due to the higher power consumption of the PSA-H_2 unit. The exergy outputs of CPSCPC-DFB-M, CPSCPC-DFB-S and CPSCPC-DFB-H are 2780.95, 2776.79 and 2910.08 MW respectively. It can be found that the total exergy output of CPSCPC-DFB-H is the highest, which is attributed to the high exergy value of H_2. Although the total exergy consumption of SCFP is low, its exergy output is also the lowest. The exergy efficiency of the four processes is shown in Fig. 5(b). Only the deep-processing part is different, while the main energy consumption parts (pyrolysis part and power generation part) are basically the same, there is little difference in exergy efficiency of the three polygeneration processes. CPSCPC-DFB-H has the highest exergy efficiency of 53.99%, while SCFP with the same power generation scale has the lowest exergy efficiency of 42.8%. The polygeneration process makes full use of the volatiles generated from the pyrolysis of low-rank coal and greatly reduces the chemical exergy loss, indicating that the dual-fluidized bed pyrolysis staged conversion polygeneration system has a higher exergy efficiency and significant advantages.

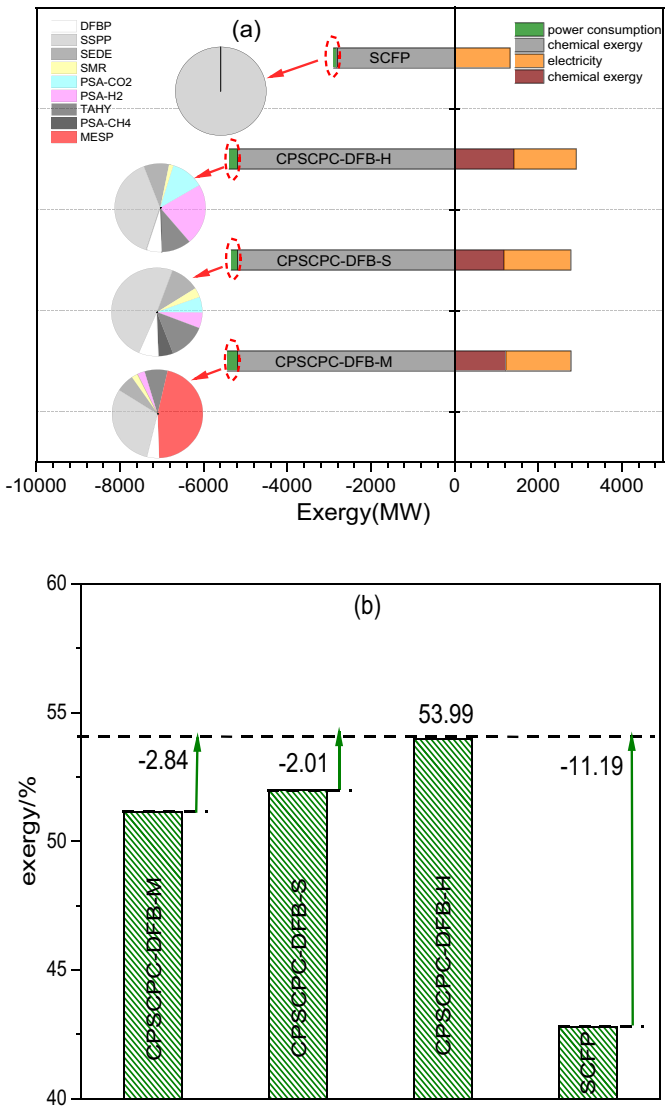

Fig. 5. Exergy distribution (a) and exergy efficiency (b) diagram.

Fig. 6 shows the energy distribution diagrams of the three processes and SCFP. The energy loss of SCFP for direct coal-fired power generation is the largest, as high as 55.60%, seriously wasting the high value-added components in coal. Through the pyrolysis staged conversion technology, the three polygeneration processes can obtain 2.71% crude phenol, 5.91% naphtha, and 7.00% diesel from coal. The 7.84% of MeOH, 7.16% of SNG and 12.16% of H_2 resources can be obtained respectively with different gas deep processing processes, and the overall energy loss is less than 50%, realizing the classification and quality utilization of coal and clean and efficient conversion. In summary, the polygeneration process is superior to the traditional ultra-supercritical power generation process.

3.3. Economic analysis of the system

3.3.1. The TCI and TPC analysis

The TCI of the four processes are shown in Fig. 7, which are 8515.04, 8453.1, 8547.9 and 5847.83 million yuan respectively. The polygeneration process requires dual-fluidized bed pyrolysis and gas deep processing equipment, so the FCI is much higher than that of SCFP. The parameters of pyrolysis part, power generation part and liquid production part for the three polygeneration systems are basically the same, so there is little difference in FCI. It can be seen from the Fig. 7(a) that CPSCPC-DFB-H has the highest FCI of 6922.95 million yuan. Compared with the other two processes, the investment is mainly increased in WGS and PSA unit. The production capacity of hydrogen in CPSCPC-DFB-H is much higher than the other two processes, so that the subsequent separation process requires more investment. Due to the simple system and single product of SCFP, the FCI is only 4736.16 million yuan, which is approximately 2100 million yuan less than the investment in the three polygeneration systems.

Fig. 7(b) shows the specific distribution of the TPC of the four processes. First, the TPC of the four processes is 3494.92, 3221.38, 3530.78 and 1744.62 million yuan respectively, and that of the polygeneration process is much higher than that of SCFP. The cost increase of the polygeneration system is attributed to C_{RM} and C_{SE}. C_{RM} includes annual coal consumption costs, electricity costs, water costs, desulfurizer costs, and catalyst costs. Since the coal consumption of the polygeneration system is much higher than SCFP, the C_{RM} is finally much higher than SCFP.

3.3.2. Analysis of IRR and PP

The IRR of the four processes are 23.24%, 21.83%, 29.52% and 17.56% respectively, indicating that all of them are economically viable as their IRR was higher than 8% (See Fig. 8). The IRR of the polygeneration process is higher than SCFP, indicating that the polygeneration process has the better economic feasibility and profitability, which can be verified by the PP. Considering the two-year construction period, CPSCPC-DFB-H with the highest investment has the shortest SPP and DPP, which are 5.06 years and 5.74 years, respectively. Hence, although the TPC and TCI of CPSCPC-DFB-H are the highest, a higher IRR shows the best economy of that. Whereas the SCFP with the least investment has longest SPP and DPP, which are 7.00 years and 8.85 years. In summary, polygeneration process achieves a higher IRR and a shorter PP by co-producing electricity, light fuel oil and chemicals.

3.3.3. Analysis of the cash flow and NPV

Cash flow analysis and NPV is an important factor in analyzing the feasibility of a project. The cash flow analysis of this work includes the total capital investment, total production cost and total income of the project during the life cycle (17 years in total). The cash flow and NPV of the four processes are shown in Fig. 9. It can be seen that the investment and cost of the three polygeneration processes are not much different, but CPSCPC-DFB-H has obvious profit advantages due to high-value hydrogen products. In the 17th year, the NPV of CPSCPC-DFB-M, CPSCPC-DFB-S, CPSCPC-DFB-H and SCFP are 8735.98, 7781.77, 14,806.2 and 3584.23 million yuan respectively, of which CPSCPC-DFB-H has the highest NPV and SCFP has the lowest NPV. Therefore, even if the total investment and cost are higher than SCFP, the economic performance of the polygeneration process is better than that of the ultra-supercritical power generation process.

3.4. Environmental assessment of system

The environmental cost results of the four systems in the whole operation process are shown in Table 9. The cost of global warming and acidification of the three polygeneration systems are much lower than those of SCFP, which is attributed to the fact that volatiles of low-rank coal are release through pyrolysis before combustion. The carbon is stored in MeOH or SNG and the sulfur is enriched. At this stage, the global warming effect caused by CO_2 has the greatest impact on the environment, so the CO_2 emissions are calculated separately as shown in Fig. 10.

The CO_2 emissions of CPSCPC-DFB-M, CPSCPC-DFB-S, CPSCPC-DFB-H and SCFP are shown in Fig. 10, which are 2.07, 2.12, 2.22 and 2.52 kg/kg_{coal} respectively. The total amount of CO_2 emitted by the polygeneration process is lower than SCFP, mainly because of the high volatile content of low-rank coal and the large amount of CO_2 generated by direct combustion. In the polygeneration process, the volatiles are

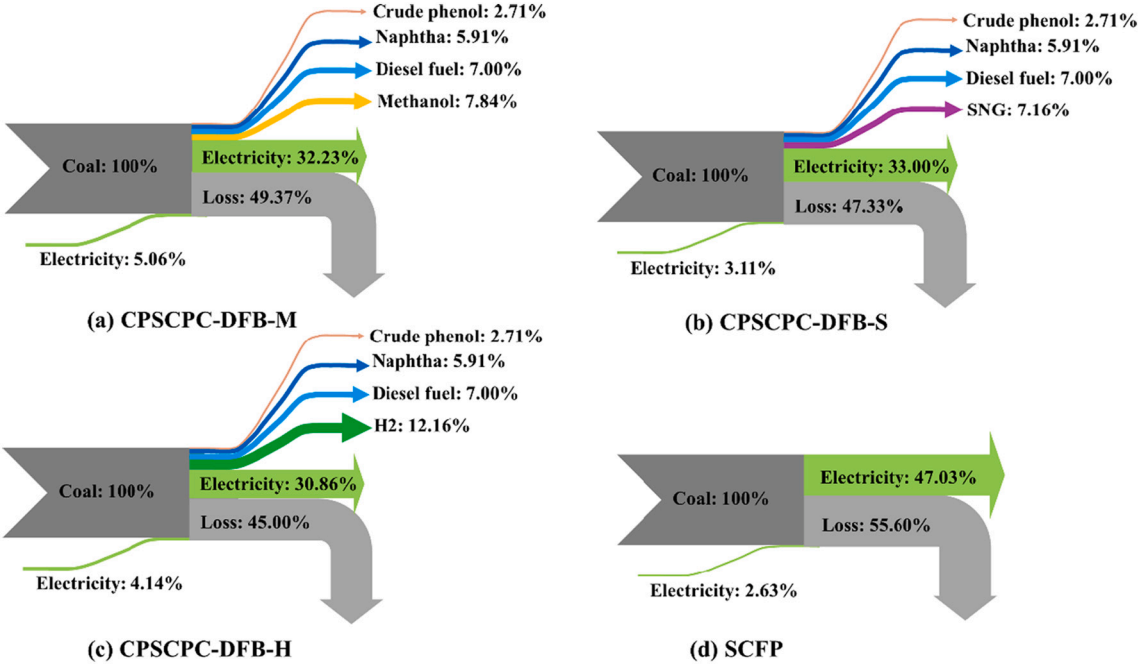

Fig. 6. The energy flow diagrams (a) CPSCPC-DFB-M, (b) CPSCPC-DFB-S, (c) CPSCPC-DFB-H, (d) SCFP.

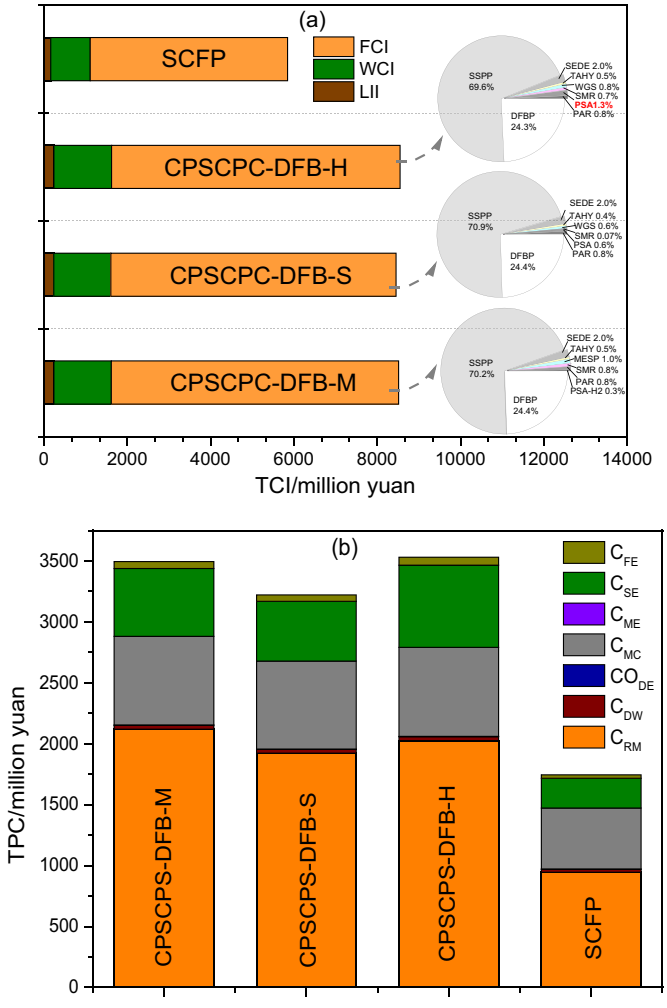

Fig. 7. The (a) TCI and (b) TPC of four process.

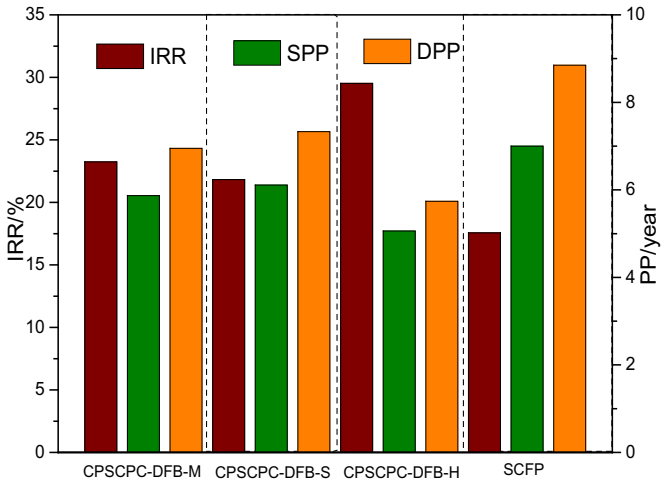

Fig. 8. The IRR and PP of the four processes.

converted into coal gas and tar components for further processing before combustion to obtain chemical and oil products, thus reducing CO_2 emissions. Compared with the polygeneration process, it can be found that CPSCPC-DFB-H emits the most CO_2 content. It can be seen from Fig. 4 that it is mainly due to the CO_2 pressure swing adsorption process and the properties of the target product (H_2).

The pyrolysis gas of polygeneration system is the main source of HC, while tar hydrogenation residue produces dangerous solid waste, so the photochemical ozone formation and solid pollution caused by the operation of the polygeneration system are higher than those of the SCFP. However, HC can be burned to provide heat in the subsequent process, and the residue can be used to produce asphalt, which can greatly reduce the environmental cost of both. In general, the environmental costs of the three polygeneration systems are lower than that of SCFP, indicating that the former have significant advantages in terms of the environment.

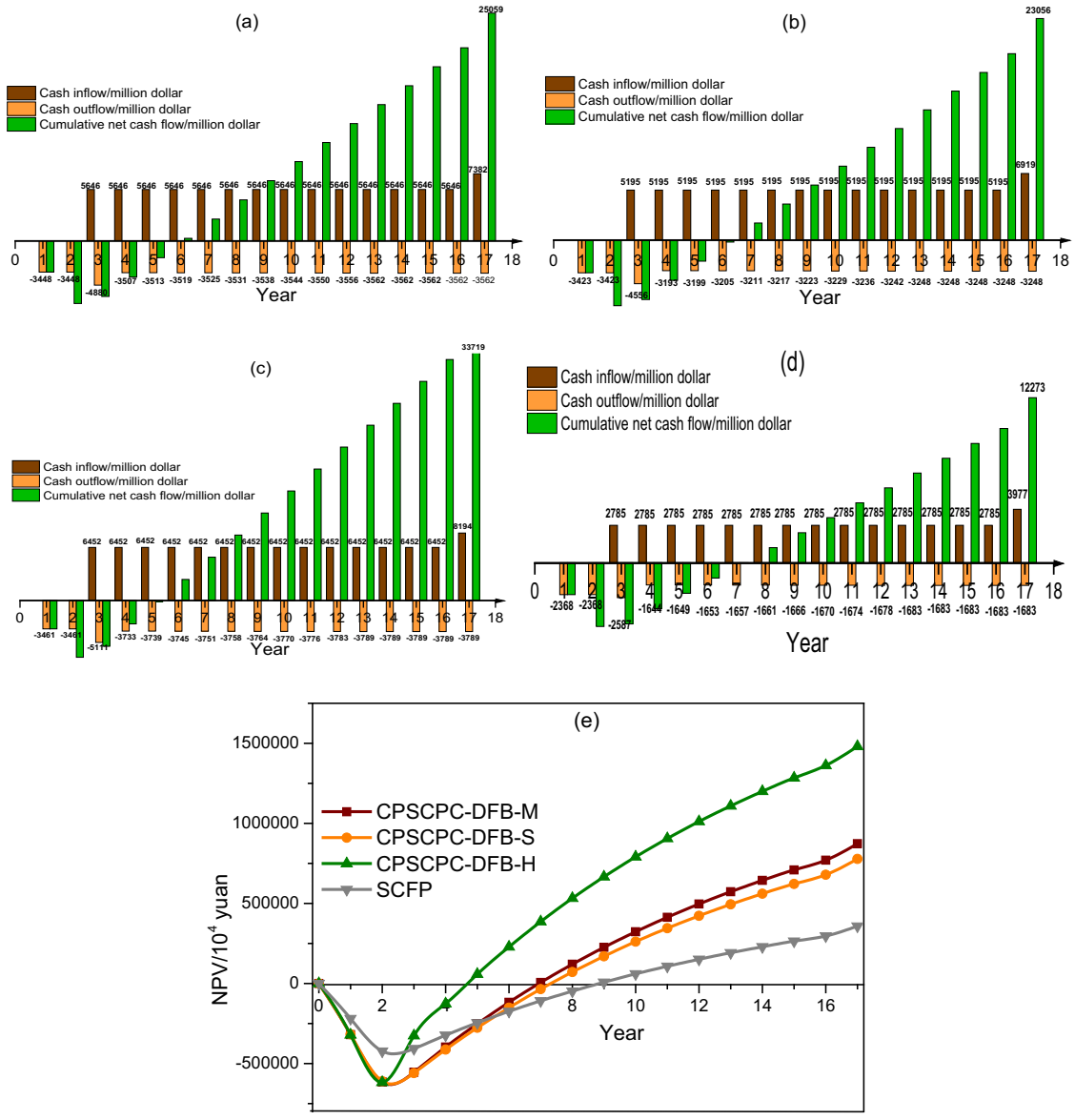

Fig. 9. Annual cash flow (a) CPSCPC-DFB-M (b) CPSCPC-DFB-S (c) CPSCPC-DFB-H (d) SCFP and (e) NPV of the four processes.

Table 9
Environmental cost of the four systems.

Impact category	pollutant	Monetary environmental value (RMB/$t_{pollutant}$)	CPSCPC-DFB-M (RMB/t_{coal})	CPSCPC-DFB-S (RMB/t_{coal})	CPSCPC-DFB-H (RMB/t_{coal})	SCFP (RMB/t_{coal})
Global warming	CO_2	80.77	167.80	171.27	179.49	203.93
	CH_4	1692.20	0.79	0.77	0.77	0
	NO_X	25,843.80	69.94	69.94	68.89	82.50
Acidification	SO_2	6057.14	24.74	26.68	24.74	96.65
	NO_X	4240.02	11.47	11.47	11.30	13.54
Photochemical ozone formation	CO	1009.52	0.0759	0.0080	0.0081	0.0054
	HC	20,190.46	35.23	35.13	35.13	0
	NO_X	3836.16	10.38	10.38	10.23	12.25
Wastewater	Effluent	3.62	0.8035	0.6303	0.5986	1.64
Solid waste	Slag	121.16	9.37	9.37	9.37	9.75
	Dangerous	4038.09	17.37	17.37	17.37	0
Total cost			347.98	353.03	357.90	420.2

3.5. Sensitivity analysis of process

The slope of the straight line reflects the degree of influence of different parameters. The price of various products is no longer the main factor affecting economic benefit for the polygeneration processes. The risk resistance of the polygeneration processes is improved through the co-production of multiple products. It can be seen from the Fig. 11 that the ART and CP are the main factors affecting the economics of the four

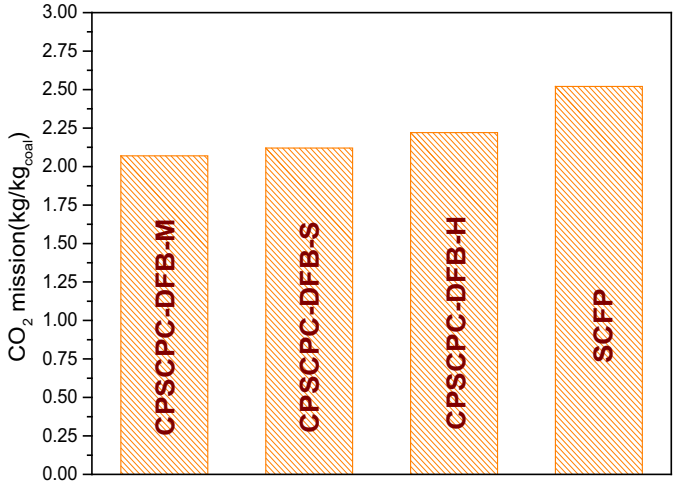

Fig. 10. CO_2 emissions of four processes.

processes.

As the ART decreases from 6250 h to 3750 h, the IRR of CPSCPC-DFB-M, CPSCPC-DFB-S, CPSCPC-DFB-H and SCFP decreases from 30.31%, 25.75%, 34.94% and 22.60% to 16.03%, 17.71%, 23.81% and 12.09%, respectively. The second factor is the CP. When the CP increases from 375 yuan/t to 625 yuan/t, the IRR of CPSCPC-DFB-M, CPSCPC-DFB-S, CPSCPC-DFB-H and SCFP decreases from 26.07%, 24.72%, 32.17% and 20.14% to 20.32%, 18.84%, 26.81% and 14.88%, respectively. However, the H_2P and CP have the same impact on the income of CPSCPC-DFB-H. On the one hand, the income brought by H_2P accounts for a large proportion of the total product income. On the other hand, the net power generation of CPSCPC-DFB-H is lower than that of CPSCPC-DFB-M and CPSCPC-DFB-S, so it is impossible to eliminate the fluctuations caused by H_2P through EP. In general, the IRR of CPSCPC-DFB-H fluctuates the least when ART, CP and H_2P change, indicating CPSCPC-DFB-H has the strongest risk resistance, broad application prospects and attractive investment. The price of various products has little effect on the overall economic benefits, indicating that polygeneration technology not only has good economic performance and broad market prospects, but also has a strong ability to resist risks.

3.6. The comprehensive influence of various properties on the system

In order to compare the comprehensive impact of technology, economy, and environmental performance on the system and clarify the relative advantages of each system, the following assumptions are made. The optimal value of each index in the process is set as 1.0, and the relative value of this index in other processes is calculated. The result is shown in Fig. 12. The larger the value of the index, the better the performance of the process in this respect. It can be seen from Fig. 12 that the comprehensive properties of the polygeneration systems are significantly better than SCFP, in terms of energy loss, exergy efficiency, CO_2 emissions, IRR and DPP. Even though the TPC and TCI of the polygeneration systems are much higher than those of SCFP, the NPV is better than SCFP. Comparing the three polygeneration systems, it is found that the TPC and CO_2 emissions of CPSCPC-DFB-H are slightly higher than those of the other two systems. The three are not much different in technology but CPSCPC-DFB-H shows an absolute advantage in economy. In the future, reducing the total investment and CO_2 emissions of polygeneration systems is essential for the sustainable

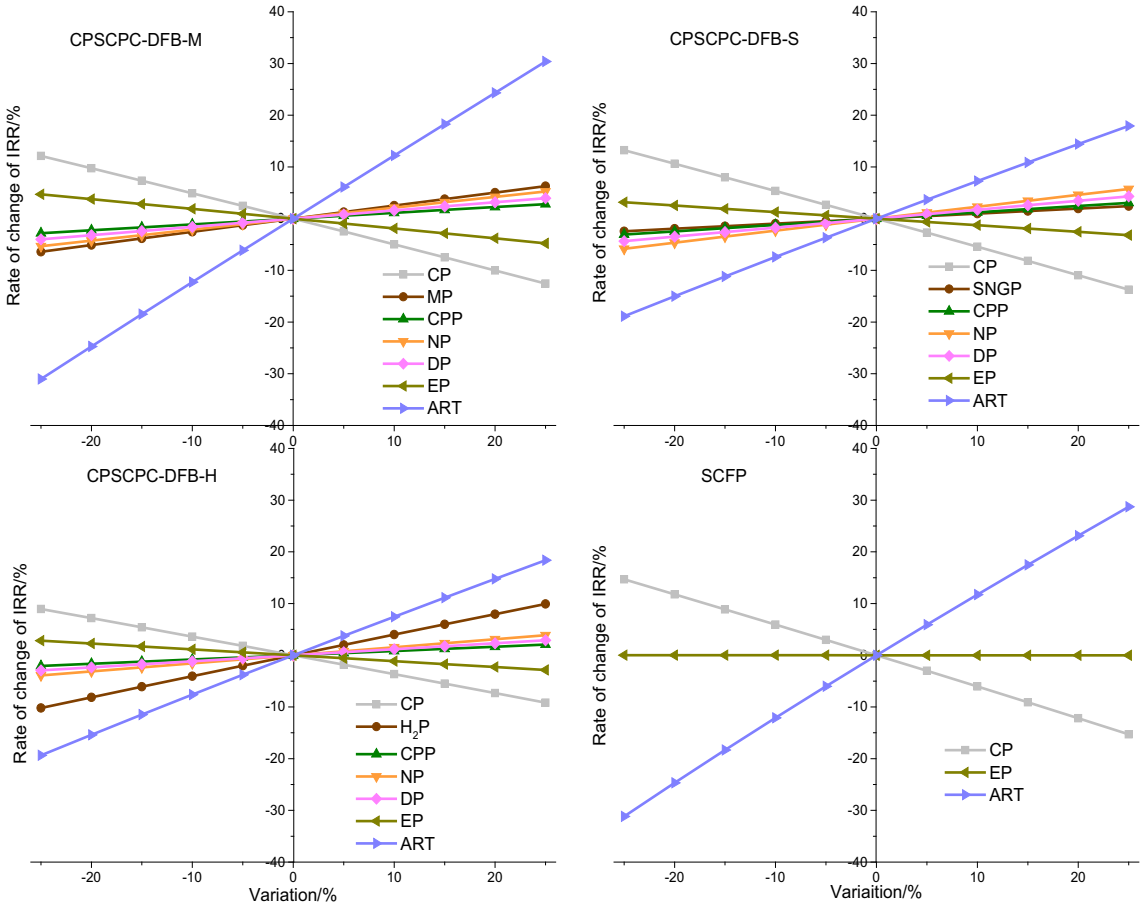

Fig. 11. The influences of sensitivity factors on the rate of change of IRR of four processes.

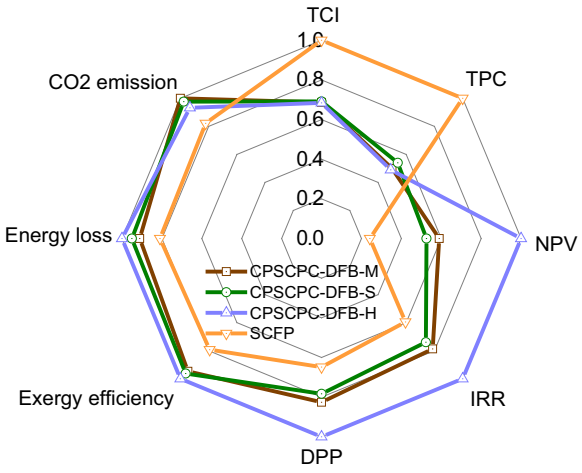

Fig. 12. The comprehensive influence of various properties on the four processes.

large-scale development of polygeneration systems.

4. Conclusions

Based on the 1MWt experiment, this work uses Aspen Plus to establish the whole process simulation and global technical and economic analysis of CPSCPC-DFB, which couples with 2 × 660 MW ultra-supercritical semi-coke powder furnace for power generation and compares with the SCFP system. The results are as follows. In terms of thermodynamics, the energy loss of CPSCPC-DFB-H is 45.00%, which is 4.37%, 2.33% and 10.60% lower than that of CPSCPC-DFB-M, CPSCPC-DFB-S and SCFP respectively. The exergy efficiency of CPSCPC-DFB-H is 53.99%, which is 2.84%, 2.01% and 11.19% higher than that of CPSCPC-DFB-M, CPSCPC-DFB-S and SCFP, respectively. In terms of economics, the annual coal consumptions of polygeneration systems are 1.31 million tons more than that of SCFP, but they have higher economic benefits. The highest FCI of CPSCPC-DFB-H is 6922.9 million yuan, which is about 2100 million yuan higher than that of SCFP, but the NPV of polygeneration process is higher than SCFP, indicating that polygeneration system has obvious benefit advantage in economy. CPSCPC-DFB-H with the highest investment has the shortest DPP of 5.74 years, while SCFP with the lowest investment has the longest DPP of 8.85 years. In terms of environmental assessment, the total CO_2 emissions of the polygeneration process are all lower than SCFP, indicating that the polygeneration process has great advantages in reducing carbon emissions. In terms of risk resistance, the ATR and CP are the main factors affecting the economic benefits of polygeneration processes. Through the dual-fluidized bed pyrolysis staged conversion technology to co-produce a variety of products, the anti-risk ability of system has been significantly improved, of which CPSCPC-DFB-H has the strongest anti-risk ability. In summary, the three polygeneration systems have obvious advantages and application prospects in the above aspects and can be flexibly selected according to market conditions and product demand.

Credit author statement

Zhu Yao: Conceptualization, Methodology, Data Curation, Writing-original draft. Li Kaikun: Visualization, Software, Investigation. Wang Qinhui: Validation, Formal analysis. Cen Jianmeng: Funding acquistion. Fang Mengxiang: Supervision. Zhongyang Luo: Writing-review&editing.

Declaration of Competing Interest

The authors declare that they have no known competing financial interests or personal relationships that could have appeared to influence the work reported in this paper.

Acknowledgments

This research was financially supported by the Fundamental Research Funds for the National Key R&D Program of China (2019YFE0100100-05).

Appendix A. Supplementary data

Supplementary data to this article can be found online at https://doi.org/10.1016/j.fuproc.2022.107217.

References

[1] S. Wang, X. Tang, J. Wang, B. Zhang, W. Sun, M. Höök, Environmental impacts from conventional and shale gas and oil development in China considering regional differences and well depth, Resour. Conserv. Recycl. 167 (2021), 105368.
[2] Q. Wang, R. Guo, Z. Wang, D. Shen, R. Yu, K. Luo, et al., Progress in carbon-based electrocatalyst derived from biomass for the hydrogen evolution reaction, Fuel. 293 (2021), 120440.
[3] J. Fan, H. Hong, H. Jin, Biomass and coal co-feed power and SNG polygeneration with chemical looping combustion to reduce carbon footprint for sustainable energy development: Process simulation and thermodynamic assessment, Renew. Energy 125 (2018) 260–269.
[4] P. Yang, X. Liang, P.J. Drohan, Using Kaya and LMDI models to analyze carbon emissions from the energy consumption in China, Environ. Ence Pollut. Res. 27 (3) (2020) 26495–26501.
[5] X. Zhu, J. Zhang, J. Yan, L. Shen, Characteristic Evaluation and Process simulation of $CuFe_2O_4$ as oxygen carriers in coal chemical looping gasification, ACS Omega. 6 (7) (2021) 4783–4792.
[6] D. Han, X. Yang, R. Li, Y. Wu, Environmental impact comparison of typical and resource-efficient biomass fast pyrolysis systems based on LCA and Aspen Plus simulation, J. Clean. Prod. 231 (2019) 254–267.
[7] C.A. Salman, M. Naqvi, E. Thorin, J. Yan, Gasification process integration with existing combined heat and power plants for polygeneration of dimethyl ether or methanol: a detailed profitability analysis, Appl. Energy 226 (2018) 116–128.
[8] S. He, S. Li, L. Gao, Proposal and energy saving analysis of novel methanol–electricity polygeneration system based on staged coal gasification method, Energy Convers. Manag. 233 (2) (2021), 113931.
[9] K. Li, Q. Wang, M. Fang, A.R. Shaikh, G. Xie, Z. Luo, Techno-Economic analysis of a coal staged conversion polygeneration system for power and chemicals production, Chem. Eng. Technol. 42 (2018) 73–88.
[10] F. Li, C. Zhao, Q. Guo, Y. Li, H. Fan, M. Guo, et al., Exploration in ash-deposition (AD) behavior modification of low-rank coal by manure addition, Energy. 208 (2020), 118293.
[11] M. Puig-Gamero, D. Pio, L. Tarelho, P. S'anchez, L. Sanchez-Silva, Simulation of biomass gasification in bubbling fluidized bed reactor using aspen plus, Energy Convers. Manag. 235 (2021) 113981.
[12] X. Zeng, J. Zhang, M.H. Adamu, F. Wang, Z. Han, Q. Zheng, et al., Behavior and kinetics of drying, pyrolysis, gasification, and combustion tested by a microfluidized bed reaction analyzer for the staged-gasification process, Energy Fuel 34 (2) (2020) 2553–2565.
[13] Q. Yi, J. Feng, B. Lu, J. Deng, C. Yu, W. Li, Energy evaluation for lignite pyrolysis by solid heat carrier coupled with gasification, Energy Fuel 27 (2013) 4523–4533.
[14] R. Zhang, Y. Chen, K. Lei, B. Ye, J. Cao, D. Liu, Thermodynamic and economic analyses of a novel coal pyrolysis–gasification–combustion staged conversion utilization polygeneration system, Asia Pac. J. Chem. Eng. 13 (2018), e2171.
[15] T. Liu, X. Zhang, Y. Liu, L. Wang, Q. Guo, Directional preparation of naphthalene oil-rich tar from Beisu low-rank coal by low-temperature catalytic pyrolysis, Carb. Res. Conv. 3 (2020) 67–75.
[16] L. Shuang, T. Cao, L. Zhang, J. Liu, X. Ren, Assessment of low-rank coal and biomass coyrolysis system coupled with gasification, Int. J. Energy Res. 44 (8) (2019) 2652–2664.
[17] A.M. Parvez, I.M. Mujtaba, P. Hall, E.H. Lester, T. Wu, Synthesis of bio-dimethyl ether based on carbon dioxide-enhanced gasification of biomass: Process simulation using Aspen Plus, Energy Technol. 4 (4) (2016) 526–535.
[18] E. Lazzaroni, M. Elsholkami, E. Martelli, A. Elkamel, Design and simulation of a petcoke gasification polygeneration plant integrated with a bitumen extraction and upgrading facility and net energy analysis - ScienceDirect, Energy. 141 (2017) 880–891.
[19] C.A. Salman, M. Naqvi, E. Thorin, J. Yan, A polygeneration process for heat, power and DME production by integrating gasification with CHP plant: Modelling and simulation study, Energy Procedia 142 (2018) 1749–1758.
[20] M.A. Adnan, A. Hidayat, M.M. Hossain, O. Muraza, Transformation of low-rank coal to clean syngas and power via thermochemical route, Energy. 1 (2021), 121505.
[21] Q. Yang, Q. Yang, S. Xu, S. Zhu, Z. Li, D. Zhang, et al., Conceptual design, techno-economic and environmental evaluation of a coal-based polygeneration process for ethylene glycol and polymethoxy dimethyl ethers production, J. Clean. Prod. 298 (2021), 126757.

[22] H. Lin, H. Jin, L. Gao, W. Han, Economic analysis of coal-based polygeneration system for methanol and power production, Energy. 35 (2) (2010) 858–863.
[23] L. Zhu, Y. He, L. Li, L. Lv, J. He, Thermodynamic assessment of SNG and power polygeneration with the goal of zero CO_2 emission, Energy. 149 (2018) 34–46.
[24] U. Ahmed, Techno-economic analysis of dual methanol and hydrogen production using energy mix systems with CO_2 capture, Energy Convers. Manag. 228 (2020), 113663.
[25] J. Chen, Y. Qian, S. Yang, Conceptual design and techno-economic analysis of a coal to methanol and ethylene glycol cogeneration process with low carbon emission and high efficiency, ACS Sustain. Chem. Eng. 8 (2020) 5229–5239.
[26] Q. Yang, S. Xu, Q. Yang, D. Zhang, S. Zhu, Optimal design and exergy analysis of biomass-to-ethylene glycol process, Bioresour. Technol. 316 (2020), 123972.
[27] G. Hu, H. Fan, Y. Liu, Experimental studies on pyrolysis of Datong coal with solid heat carrier in a fixed bed, Fuel Process. Technol. 69 (3) (2001) 221–228.
[28] S. Quan, L. Shi, B. Zhou, Z. Liu, Q. Liu, Study of temperature variation of walnut shell and solid heat carrier and their effect on primary pyrolysis and volatiles reaction, Fuel. 292 (5) (2021), 120290.
[29] X.-H. Li, J.-S. Ma, L.-L. Li, B.-F. Li, J. Feng, W. Turmel, et al., Semi-coke as solid heat carrier for low-temperature coal tar upgrading, Fuel Process. Technol. 143 (2016) 79–85.
[30] G. Hu, X. Gong, H. Hao, H. Fan, W. Zheng, Experimental studies on flow and pyrolysis of coal with solid heat carrier in a modified rotating cone reactor, Chem. Eng. Process. Process Intensif. 47 (2008) 1777–1785.
[31] M. Wang, L. Jin, Y. Li, J. Wang, X. Yang, H. Hu, In Situ Catalytic upgrading of coal pyrolysis tar over carbon-based catalysts coupled with CO_2 reforming of methane, Energy Fuel 31 (9) (2017) 9356–9362.
[32] L. Jin, X. Bai, L. Yang, D. Chan, L. Xian, In-situ catalytic upgrading of coal pyrolysis tar on carbon-based catalyst in a fixed-bed reactor, Fuel Process. Technol. 147 (2016) 41–46.
[33] Q. Zhou, T. Zou, M. Zhong, Y. Zhang, R. Wu, S. Gao, et al., Lignite upgrading by multi-stage fluidized bed pyrolysis, Fuel Process. Technol. 116 (2013) 35–43.
[34] Z. Guo, Q. Wang, M. Fang, Z. Luo, K. Cen, Thermodynamic and economic analysis of polygeneration system integrating atmospheric pressure coal pyrolysis technology with circulating fluidized bed power plant, Appl. Energy 113 (2014) 1301–1314.
[35] M. Gao, G. Chen, X. Zhang, S. Shi, L. Wu, Simulation research of the product separation process for coal tar hydrogenation with heterogeneous suspended bed, Coal Chem. Ind. 98 (3) (2013) 411–428.
[36] H. Huang, S. Yang, Design concept for coal-based polygeneration processes of chemicals and power with the lowest energy consumption for CO_2 capture, Comp. Aid. Chem. Eng. 44 (2018) 1381–1386.
[37] J. Parraga, K. Khalilpour, A. Vassallo, Polygeneration with biomass-integrated gasification combined cycle process: review and prospective, Renew. Sust. Energ. Rev. 92 (2018) 219–234.
[38] R.S. El-Emam, I. Dincer, G.F. Naterer, Energy and exergy analyses of an integrated SOFC and coal gasification system, Int. J. Hydrog. Energy 37 (2) (2012) 1689–1697.
[39] M.S. Herdem, S. Farhad, I. Dincer, F. Hamdullahpur, Thermodynamic modeling and assessment of a combined coal gasification and alkaline water electrolysis system for hydrogen production, Int. J. Hydrog. Energy 39 (2014) 3061–3071.
[40] B. Ye, B. Shi, M. Shi, L. Zhang, R. Zhang, Process simulation and comprehensive evaluation of a system of coal power plant coupled with waste incineration, Waste Manag. Res. 39 (2020) 828–840.
[41] S. Li, L. Gao, X. Zhang, H. Lin, H. Jin, Evaluation of cost reduction potential for a coal based polygeneration system with CO_2 capture, Energy. 45 (1) (2012) 101–106.
[42] C. Ye, Q. Wang, Y. Zheng, G. Li, Z. Zhang, Z. Luo, Techno-economic analysis of methanol and electricity poly-generation system based on coal partial gasification, Energy. 185 (2019) 624–632.
[43] D.P. Hanak, S. Michalski, V. Manovic, Supercritical CO_2 cycle for coal-fired power plant based on calcium looping combustion, Therm. Sci. Eng. Progr. 20 (2020), 100723.
[44] J. Xiao, L. Shen, Y. Zhang, J. Gu, Integrated analysis of energy, economic, and environmental performance of biomethanol from rice straw in China, Ind. Eng. Chem. Res. 48 (22) (2009) 9999–10007.